

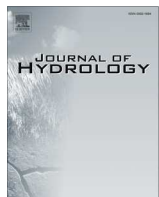


ELSEVIER

Contents lists available at ScienceDirect

# Journal of Hydrology

journal homepage: [www.elsevier.com/locate/jhydrol](http://www.elsevier.com/locate/jhydrol)



## Research papers

# Upland and in-stream controls on baseflow nutrient dynamics in tile-drained agroecosystem watersheds



William I. Ford <sup>a,\*</sup>, Kevin King <sup>b</sup>, Mark R. Williams <sup>c</sup>

<sup>a</sup> *Biosystems and Agricultural Engineering, University of Kentucky, Lexington, KY, United States*

<sup>b</sup> *USDA-ARS Soil Drainage Research Unit, Columbus, OH, United States*

<sup>c</sup> *USDA-ARS National Soil Erosion Research Laboratory, West Lafayette, IN, United States*

## ARTICLE INFO

### Article history:

Received 3 May 2017

Received in revised form 24 October 2017

Accepted 3 December 2017

Available online 6 December 2017

This manuscript was handled by L. Charlet, Editor-in-Chief, with the assistance of Fereidoun Rezanezhad, Associate Editor

### Keywords:

Water quality

Nutrients

Drainage

Agriculture

Time-series

CEAP

## ABSTRACT

In landscapes with low residence times (e.g., rivers and reservoirs), baseflow nutrient concentration dynamics during sensitive timeframes can contribute to deleterious environmental conditions downstream. This study assessed upland and in-stream controls on baseflow nutrient concentrations in a low-gradient, tile-drained agroecosystem watershed. We conducted time-series analysis using Empirical mode decomposition of seven decade-long nutrient concentration time-series in the agricultural Upper Big Walnut Creek watershed (Ohio, USA). Four tributaries of varying drainage areas and three main-stem sites were monitored, and nutrient grab samples were collected weekly from 2006 to 2016 and analyzed for dissolved reactive phosphorus (DRP), nitrate-nitrogen ( $\text{NO}_3\text{-N}$ ), total nitrogen (TN), and total phosphorus (TP). Statistically significant seasonal fluctuations were compared with seasonality of baseflow, watershed characteristics (e.g., tile-drain density), and in-stream water quality parameters (pH, DO, temperature). Findings point to statistically significant seasonality of all parameters with peak P concentrations in summer and peak N in late winter-early spring. Results suggest that upland processes exert strong control on DRP concentrations in the winter and spring months, while coupled upland and in-stream conditions control watershed baseflow DRP concentrations during summer and early fall. Conversely, upland flow sources driving streamflow exert strong control on baseflow  $\text{NO}_3\text{-N}$ , and in-stream attenuation through transient and permanent pathways impacts the magnitude of removal. Regarding TN and TP, we found that TN was governed by  $\text{NO}_3\text{-N}$ , while TP was governed by DRP in summer and fluvial erosion of P-rich benthic sediments during higher baseflow conditions. Findings of the study highlight the importance of coupled in-stream and upland management for mitigating eutrophic conditions during environmentally sensitive timeframes.

© 2017 Elsevier B.V. All rights reserved.

## 1. Introduction

Increases in systematic tile-drainage in low-gradient agricultural landscapes have significantly impacted watershed hydrology and nutrient fate and transport over the past 50 years (Blann et al., 2009; King et al., 2014a; Christianson et al., 2016). For instance, in the Western Lake Erie Basin, increasing occurrence of harmful cyanobacteria algal blooms (HABs) has been linked to increases in dissolved reactive phosphorus (DRP) loading, potentially caused by several compounding factors including increased drainage intensity (Smith et al., 2015). Much emphasis has been placed on nutrient loading dynamics during storm flows given the disproportionate control of events on nutrient fluxes (e.g., Sharpley et al.,

2008). Notwithstanding the significance of large nutrient fluxes during storm events, tile drainage can be a major component of stream baseflow (Shilling and Helmers, 2008; King et al., 2014a, b) and baseflow nutrient concentrations (Schilling and Zhang, 2004). Baseflow nutrient concentrations, which constitute less than 10% of annual nutrient loads, may play a significant role in HAB formation in small lakes and riverine environments given the low water retention times in these systems (Shore et al., 2017). In order to identify the most effective management strategies at a watershed-scale, a need exists to better understand the underlying upland and in-stream mechanisms controlling nutrient concentrations in tile-drained landscapes.

Intra-annual variability in baseflow stream nitrate ( $\text{NO}_3\text{-N}$ ) concentration has been reported due to seasonal differences in the rates of in-stream and riparian biochemical reactions and time-varying contributions of drainage sources (Pionke et al., 1999; Peterson et al., 2001; Mulholland et al., 2008; Griffiths et al.,

\* Corresponding author at: Biosystems and Agricultural Engineering, University of Kentucky, Lexington, KY 40546, United States.

E-mail address: [bill.ford@uky.edu](mailto:bill.ford@uky.edu) (W.I. Ford).

2012; Exner-Kittridge et al., 2016; Ford et al., 2017a). As recently highlighted in Exner-Kittridge et al. (2016), stream baseflow  $\text{NO}_3\text{-N}$  concentrations have been observed to increase in the winter and decrease in the summer within temperate tile-drained landscapes. Denitrification and algal uptake are pronounced in the summer and can deplete  $\text{NO}_3\text{-N}$  resulting in either permanent or transient removal of N; yet, algal assimilation is often neglected in watershed mass-balance calculations (Mulholland et al., 2008; Ford et al., 2017a). The source of  $\text{NO}_3\text{-N}$  and flow pathway for delivery may also influence concentrations in these watersheds. Nitrate may originate from subsurface seepage in the variably saturated vadose zone and/or deeper saturated aquifers (Exner-Kittridge et al., 2016). High stream  $\text{NO}_3\text{-N}$  concentrations in winter may reflect the prominence of N-laden shallow vadose-zone water from tile drains during wet antecedent conditions. Conversely, low stream  $\text{NO}_3\text{-N}$  concentrations in summer may reflect minimal contributions of systematic drainage (Williams et al., 2015a) and higher saturated zone flow from deeper aquifers that are depleted in N due to extended residence time for denitrification. While both in-stream and upland processes likely exert some control on stream  $\text{NO}_3\text{-N}$  concentration, the extent to which processes control  $\text{NO}_3\text{-N}$  at increasing watershed scales is not well understood.

While dissolved reactive phosphorus (DRP) trends from long-term records have shown mixed results in terms of seasonal max-min dynamics, studies specifically targeting baseflow have shown peak DRP concentrations during summer; however, the mechanisms controlling these dynamics are not well-understood (Mulholland and Hill, 1997; Pionke et al., 1999; Stow et al., 2015; Shore et al., 2017). Elevated DRP concentration in summer could reflect several potential in-stream and upland pathways. Regarding upland soil drainage, greater DRP could reflect enhanced weathering and dissolution of phosphorus (P) bearing substrata, evapotranspiration in the vadose zone, or enhanced mineralization of organic matter (Jarvie et al., 2014; Hartmann et al., 2014; Ford et al., 2015a). In many agricultural watersheds, soil bound P tends to be highly stratified, with elevated levels in surface soils; hence, we would not suspect high connectivity to subsurface drainage for baseflow concentrations (King et al., 2014a,b; Baker et al., 2017). However, macropore flow through desiccation cracks could resupply shallow aquifers below tile-drains with enriched P concentrations during dry summer months, which is subsequently leached to the stream (Williams et al., 2016; Ford et al., 2017b). In streams, elevated DRP concentrations could be associated with enhanced release of DRP by polyphosphate accumulating organisms in benthic biofilms, dissolution of phosphate precipitates (analogous to soil drainage), or desorption of legacy sediment P immobilized in transient storage zones (Wang et al., 2008; Jarvie et al., 2014; Wu et al., 2014; Saia et al., 2017).

The objective of the present study was to utilize ambient long-term records of nutrient concentrations (namely  $\text{NO}_3\text{-N}$ , DRP, total N (TN), and total P (TP)) to identify upland and in-stream controls on nutrient concentrations at baseflow conditions. We focus on tile-drained midwestern watersheds given the rampant acute and chronic nutrient flux problems that are well documented in these landscapes. Specifically, we aim to identify and discuss the following questions: (1) do seasonal baseflow nutrient dynamics agree with common perceptions?; (2) to what extent are watershed fluxes reflective of in-stream and upland controls?; and (3) what are the environmental and management implications for tile-drained agroecosystems? To answer these questions, we use a 10-year dataset and time series analysis of longitudinal watershed data in the Upper Big Walnut Creek (UBWC) USDA benchmark watershed located in central Ohio, USA and compare the data to critical upland drainage nutrient concentrations and in-stream water quality indicators.

## 2. Methods

### 2.1. Study sites

The HUC 11 Upper Big Walnut Creek watershed (HUC 05060001-130) located in central Ohio, USA is a benchmark United States Department of Agriculture (USDA) Agricultural Research Service (ARS) research watershed and is one of the 24 watersheds selected for the Conservation Effects Assessment Project, CEAP (Arnold et al., 2014; Fig. 1). The watershed drains through the Hoover Reservoir, which is a major drinking water source for the Columbus, Ohio metropolitan area (Richardson et al., 2008; Fig. 1). The UBWC has a drainage area of 492 km<sup>2</sup> and is predominantly (~60%) composed of cropland for production agriculture with major crops including corn, soybeans, and wheat (King et al., 2008). Extensive tile drainage networks in the watershed stem from fine, clayey soil texture which primarily consist of Bennington-Pewamo-Cardington soil associations (60%) (Table 1; King et al., 2008). We refer the reader to King et al. (2008) for further site characterization.

Eight HUC 12 watersheds are nested within the UBWC basin, of which four (T-1, T-2, T-3, and T-4) were monitored from 2006 through 2016. Three additional sites located on the main-stem (MS-1, MS-2, and MS-3) of the watershed were also monitored and each main-stem monitoring site incorporates an additional HUC 12 watershed. A U.S. Geological Survey real-time gauging station co-located at MS-2 (USGS 03228300) has historical water quality data spanning much of the nutrient data collection time-frame (late 2007-Present). Hydrologic and water quality data at MS-2 includes flowrate, water temperature, specific conductivity, dissolved oxygen (DO), and pH. Topographic, drainage, soil, and land use characteristics of the HUC 12 watersheds are summarized in Table 1. Information in Table 1 for the main-stem sites reflect the additional drainage area added at the monitoring location. Two small municipal wastewater treatment facilities are in the UBWC watershed between MS-2 and MS-3 and have maximum allowable loadings of 0.617 kg P/km<sup>2</sup>/yr and 2.18 kg N/km<sup>2</sup>/yr (as ammonium) respectively per EPAs Discharge Monitoring Report Pollutant Loading Tool (U.S. EPA, 2017). Such loadings are small in comparison with agricultural watershed P loadings reported in the UBWC of 98 kg P/km<sup>2</sup>/yr.

### 2.2. Data collection and analysis

Weekly grab samples were collected from the middle of the stream at each of the seven study locations using standard U.S. EPA protocol for collection and preservation of water samples for N and P analysis (U.S. EPA, 1983). Water level at each of the monitoring locations was also measured at the time of sample collection. Water samples were immediately brought back to the lab and refrigerated (4 °C) until they were filtered through 0.45 µm Glass Microfibre filters. DRP and  $\text{NO}_3\text{-N}$  concentrations in filtered samples were determined colorimetrically by flow injection analysis using a Quik Chem 8000 FIA Automated Ion Analyzer (Lachat Instruments). Total N and TP analyses were performed on unfiltered samples following alkaline persulfate oxidation (Koroleff, 1983). All water samples were analyzed within 28 days following collection.

### 2.3. Statistical analysis

Empirical mode decomposition was selected as the preferred method for the analysis since the method is purely empirical (e.g., does not use sine-cosine functions), makes no limiting assumptions about the dataset, can be applied to a wide class of

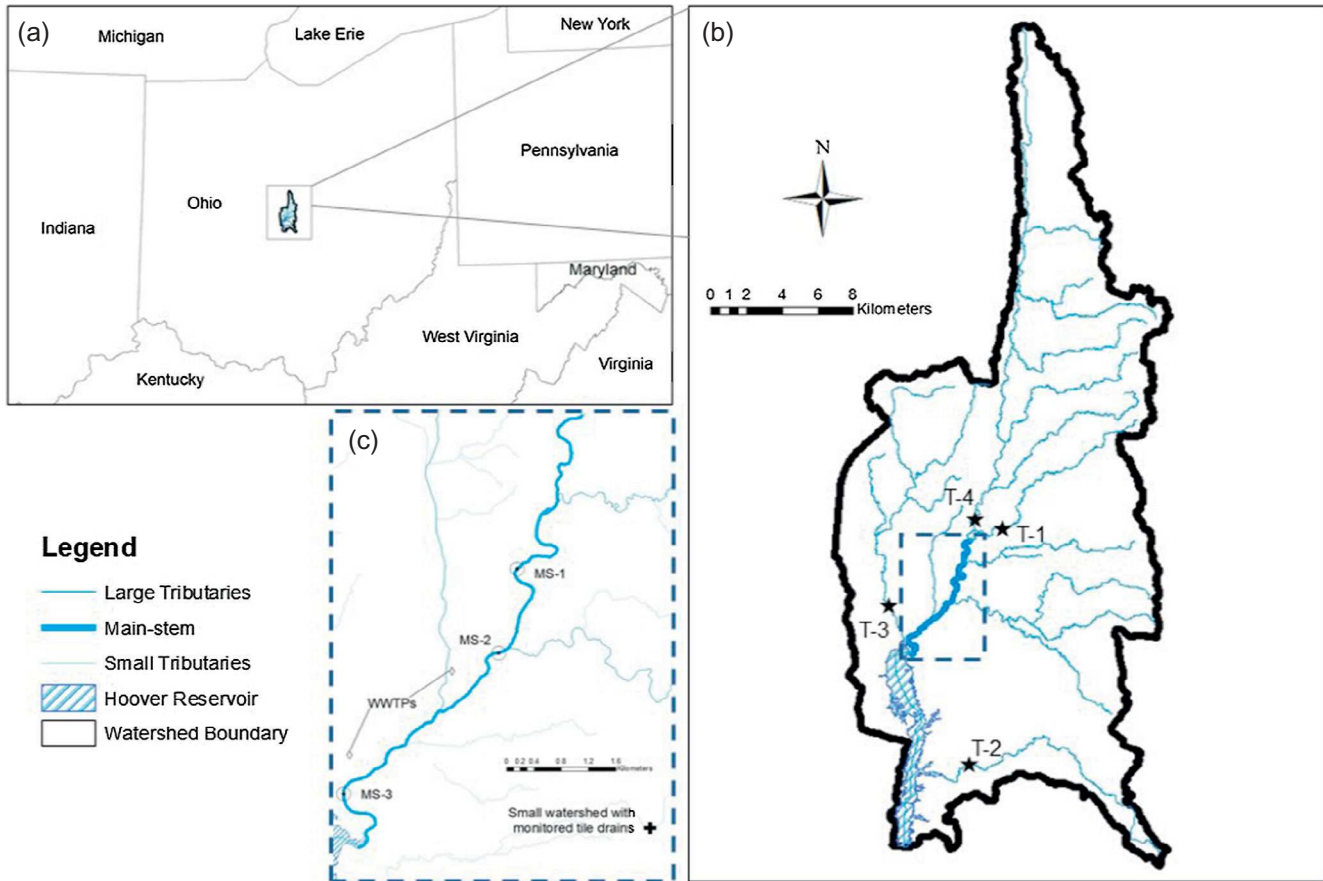


**Fig. 1.** Study site map including a) location of the UBWC watershed in central Ohio, b) UBWC watershed boundary with defined tributary network and monitoring locations (T-1 to T-4) and main-stem stream network, and c) main-stem sampling locations (MS-1 to MS-3) and supplemental points of interest. A USGS gauging station (03228300) is co-located at MS-2.

**Table 1**  
Watershed characteristics of monitoring sites in the Upper Big Walnut Creek. Information for the main-stem sites reflect the additional contributing area since the nearest upstream monitoring stations.

Watershed Properties	Attribute	T-1	T-2	T-3	T-4	M2-1	MS-2	MS-3
Geometry	Drainage Area (km <sup>2</sup> )	34.7	44.6	84.8	142.8	26.0	59.0	22.3
	Watershed Relief (m)	107.0	100.0	70.0	128.0	81.0	79.0	57.0
	Watershed Slope (%)	2.9	2.6	3.4	3.9	2.6	2.6	3.2
	Stream Slope (%)	0.37	0.43	0.30	0.13	0.43	0.30	0.27
Tile Drainage	Tiled Drainage Area (%)	44.8	39.1	34.1	16.1	65.3	59.2	41.2
Soil Drainage capacity	Very poor (%)	31.0	37.0	20.0	15.0	31.0	30.0	25.0
	Somewhat poor (%)	50.0	49.0	38.0	29.0	48.0	46.0	29.0
	Moderately well (%)	16.0	12.0	38.0	50.0	19.0	22.0	43.0
	Well (%)	3.0	2.0	4.0	6.0	2.0	2.0	3.0
Land use 2005[2013]	Agricultural (%)	58.5[57.5]	63.0[62.5]	48.9[46.5]	48.3[47.6]	51.8[51.0]	54.8[54.1]	49.1[47.9]
	Urban (%)	21.7[22.8]	26.1[26.9]	32.9[35.6]	22.5[23.8]	21.5[22.8]	21.5[22.6]	35.3[36.6]
	Woodland (%)	19.2[19.1]	10.9[10.7]	17.5[17.2]	29.2[28.6]	26.1[25.7]	22.9[22.5]	14.4[14.3]
	Shrubland (%)	0.6[0.6]	0[0]	0.8[0.7]	0[0]	0.6[0.5]	0.8[0.8]	1.2[1.2]

signals, and can be used as an *a posteriori* approach, which is ideal for an exploratory analysis (Huang et al., 1998; Wu et al., 2007; Ford et al., 2015b). The method has been broadly applied to a wide range of environmental signals, most relevant to this study include applications to sediment carbon and N elemental and isotopic signatures (Ford et al., 2015b) and climate data (Wu et al., 2007). For the analyses in the current study, datasets were assumed to be non-linear, non-stationary, and to have non-parametric distributions. Therefore, all datasets were first log-transformed due to their non-normal skewed distributions so that the noise of the stochastic event-event variability did not mask significant trends (Venier

et al., 2012). Exploratory time-series analysis was performed on the decade long nutrient datasets at all monitoring locations within the UBWC watershed. Empirical mode decomposition (EMD) was used to decompose the nutrient time series into intrinsic mode functions (IMFs) (Huang et al., 1998; Wu et al., 2007).

Intrinsic mode functions are a finite series of amplitude and frequency modulated, oscillatory functions in which lowest frequency IMF is identified as the base trend and the highest frequency trend is considered noise for well-sampled datasets (Wu et al., 2007). Empirical mode decomposition was conducted utilizing a six step iterative procedure as summarized in Ford et al. (2015b), in which

(1) local maxima and minima are identified in the time series, (2) cubic spline interpolation signals are computed to create upper and lower envelopes, (3) upper and lower envelopes are averaged, (4) the average envelope is subtracted from the signal (related to the current iteration), (5) the process is repeated until the averaged envelope converges to a stated threshold, (6) the resulting IMF is subtracted from the original dataset to create a new time series and steps 1–5 are repeated until all extremes are removed.

We compiled a previously published code in Matlab that performs EMD and generates IMFs for each site (Rato et al., 2008). We performed statistical significance tests to test the hypothesis that IMFs of the dataset were statistically different from white noise IMFs (Wu and Huang, 2004; Wu et al., 2007; Ford et al., 2015b). A log-log plot of variance versus mean period was plotted for each IMF and tested against a confidence interval for white noise (Wu and Huang, 2004). The highest frequency trend was used as the basis for noise and a negative linear relationship of  $\log(\text{Var})$  versus  $\log(\text{Period})$ , with a slope of  $-1$ , was plotted with upper and lower bounds for the confidence interval being represented with  $\log_{10}(\text{Var}) \pm \log_{10}(3)$ . The protocol allotted three standard deviations for confidence bounds for noise. Intrinsic mode functions with frequencies that plot outside the specified variance range are statistically differentiable from white noise and thus are expected to have some physical meaning. Aggregation of statistically significant trends for IMFs for the EMD results was conducted by combining IMFs at environmentally relevant timescales. For the present study, we focus on the seasonal timescale given the implications for seasonal eutrophication and HABs. Statistically significant frequencies between 0.7 and 1.3 years were included as a seasonal fluctuation because trends may not have pronounced peaks in some years (resulting in a frequency  $>1$  year), or may experience a secondary oscillation in some years (resulting in a frequency  $<1$  year). If such a phenomenon is commonly occurring, leading to frequencies outside of the specified bounds, we suggest that the result is likely due to a non-seasonal fluctuation. For the results, we define any statistically significant IMF as a “trend” throughout the remainder of the manuscript.

Non-parametric statistical tests, linear regression, and explanatory visual statistical plots were utilized to compare nutrient datasets between sites. Box-and-whisker plots were used to visualize distributions and were generated in SigmaPlot 13. Given the skew of the data, the y-axis was plotted on a log-scale. Independence of individually collected samples was assumed and statistical tests were performed in the statistical package *Sigmastat 13*. Specifically, the Mann-Whitney Rank Sum test was utilized to determine statistically significant differences in median values for the datasets. The Rank Sum Test is nonparametric, thus does not require assuming data normality or equal variance. A significance level of  $\alpha = 0.05$  was selected for testing the null hypothesis that the two samples were not drawn from the same populations. Specifically, we were interested in testing how the main-stem sites compared to tributary ranges.

### 3. Results

#### 3.1. Exploratory statistics

Median concentrations in the tributaries ranged from 0.6–1.5 mg/L for  $\text{NO}_3\text{-N}$ , 1.0–2.2 mg/L for TN, 0.01–0.06 mg/L for DRP, and 0.05–0.09 mg/L for TP (Fig. 2). In general, T-2 had significantly higher ( $P < .001$ ) median values relative to other tributaries for all water quality constituents (Table 2). T-1 had the lowest total nutrient concentrations, while T-3 had the lowest dissolved nutrient concentrations, reflecting higher sediment-bound nutrient constituents in T-3 relative to T-1. Statistical results in Table 2 and

Fig. 2 show that median values of MS-1 and MS-2 were not significantly greater than the maximum tributary median or less than the minimum tributary median for any nutrient concentration. Regarding MS-3, results for both  $\text{NO}_3\text{-N}$  and TN show that the median was not statistically differentiable from the maximum tributary, while DRP was significantly greater than both the maximum and minimum tributary medians. As shown in Table 1, MS-3 only drains an additional 22 km<sup>2</sup> (approximately 10% of the total drainage area).

#### 3.2. Empirical mode decompositions

Results of the EMD statistical analysis for monitored watersheds highlight significant trends at multiple timescales (Table 3; Figs. 3 and 4). Intra-annual trends (<6-month frequency) rarely occurred; however, they were found for several parameters at MS-2 including flow,  $\text{NO}_3\text{-N}$ , and TN. Results of EMD analysis showed that statistically significant seasonal trends were common among all sites and measured parameters. The only datasets without seasonal trends were T-3 and MS-1 ( $\text{NO}_3\text{-N}$ ), T-3 (DRP), and T-2 (TP). We note that seasonal trends reflect baseflow conditions based on results of the time-series analysis of flow depth. Longer-term trends (>2 years) were less common but were found for flow depths at most sites, all sites for DRP and TP, and approximately half the sites for  $\text{NO}_3\text{-N}$  and TN.

Nevertheless, visual observations of seasonal trends describe much of the cumulative statistically significant variability in the dataset, especially for P (Figs. 3 and 4). This result is evidenced by direct comparison of the “Sum of all significant IMFs” with the “Seasonal + Residual IMFs”. For  $\text{NO}_3\text{-N}$  and TN, intra-annual trends become an important descriptor of total variability at some stations (namely T-2, T-3 and MS-2). For instance,  $\text{NO}_3\text{-N}$  at MS-2 shows frequencies of approximately six months in the first half of the year throughout the monitored timeframe. This was likely attributed to N fertilizer applications which are commonly applied at time of planting and side-dressed during the growing season. Multi-year trends rarely appeared and were less commonly significant as compared to seasonality. It is likely that multi-year trends were associated with compounding factors such as annual precipitation (wet year – dry year), and predominant crop rotations; however, the imprint of these fluctuations was relatively minor compared to seasonal and intra-annual variability. As such, we do not emphasize multi-year, or intra-annual trends in the subsequent discussion of EMD results.

Differences in seasonal maximums-minimums for N and P were also observed (Figs. 3 and 4). In general, T-1, T-2, T-3, T-4, MS-1 and MS-2 showed consistent patterns (albeit different magnitudes) of max-min timing for both N and P. Given this result, we place emphasis on MS-2 since seasonal trends can be compared to water quality data at the co-located USGS gauging station. Peak N concentrations were often found in spring (April–June) and minimum N concentrations were found in mid-summer to early-fall (August–October). The timing and magnitude of seasonal trends for  $\text{NO}_3\text{-N}$  and TN were similar and will be further discussed in Section 3.3. Phosphorus seasonal trends were generally inversely related to N, with minimum P concentrations generally found in early- to mid-spring (April–June) and maximum values typically found in mid-summer to early-fall (August–October). Dissolved reactive P and TP deviated in seasonal trends at some locations. For instance, we observed a seasonal trend for TP but not DRP at site T-3 (Table 3; Fig. 4) in which the timing was more reflective of N dynamics with maximums in spring and minimums in late summer.

Longitudinal variability in seasonal trends of the main-stem sites showed increasing downstream nutrient concentrations that periodically exceed ranges of seasonal trends observed in

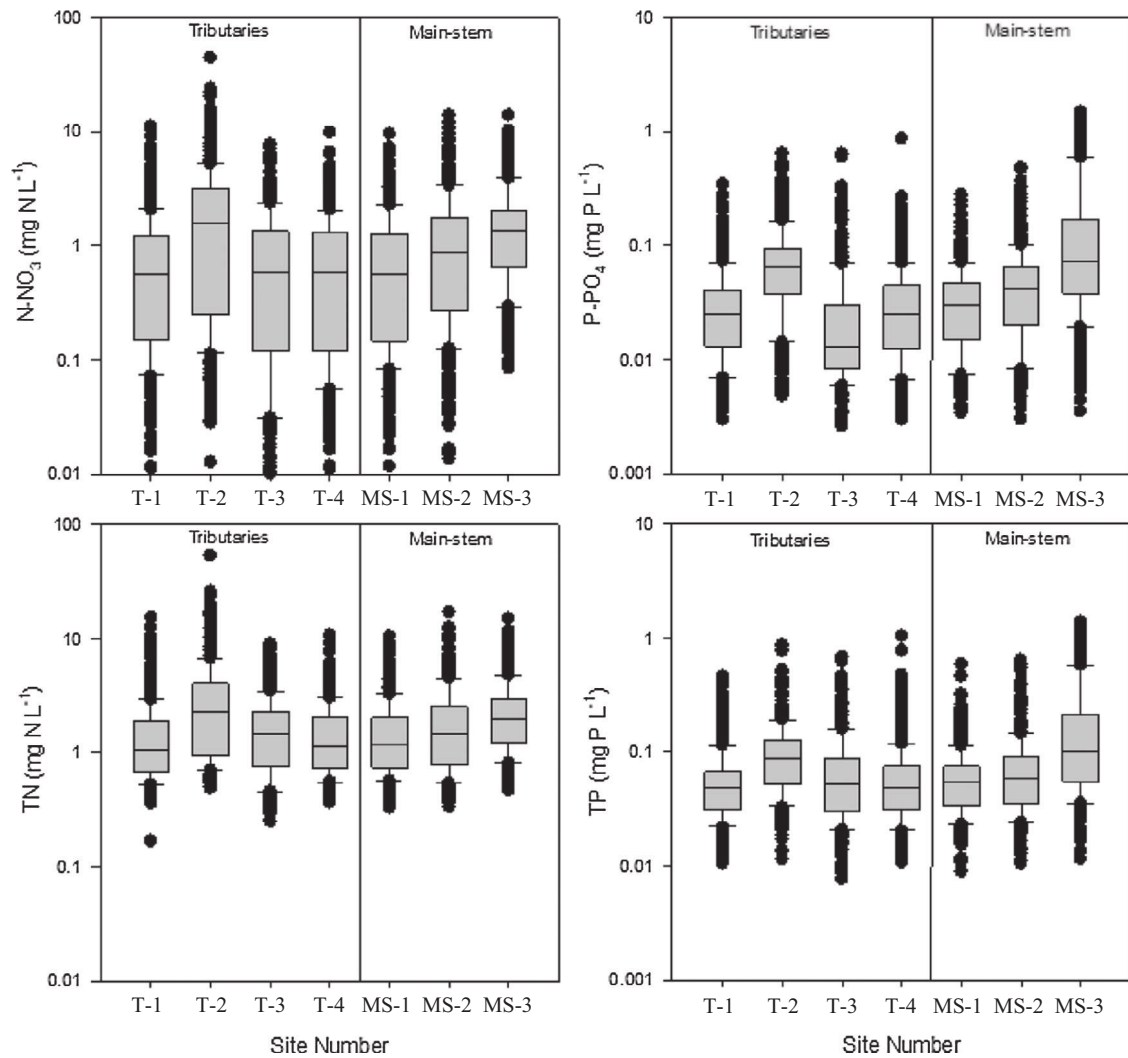


**Fig. 2.** Box and whisker plots of nitrate-nitrogen, phosphate-phosphorous, total nitrogen and total phosphorus concentrations for each of the monitored HUC 12s in the Upper Big Walnut Creek.

**Table 2**

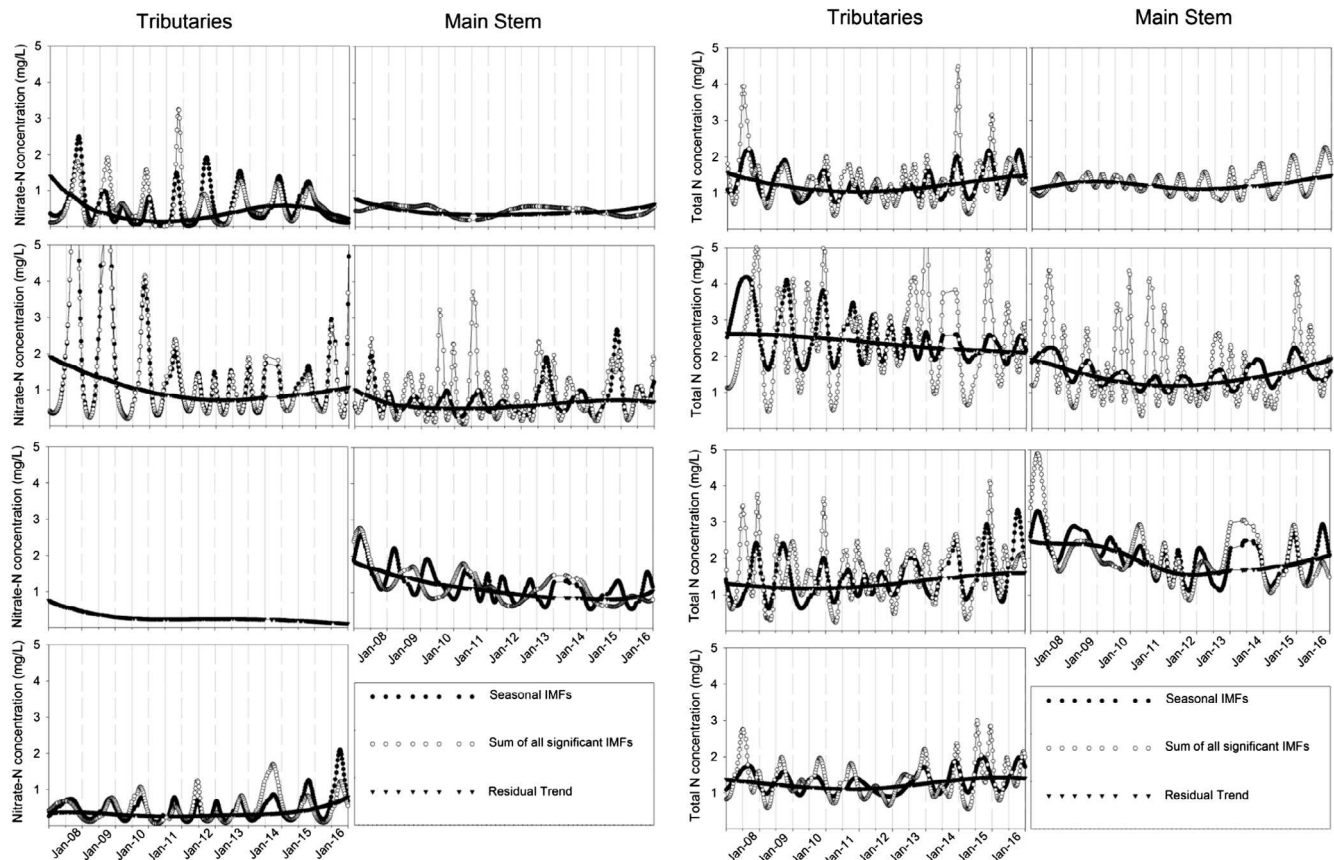
Statistical significance test results comparing main-stem sites to maximum and minimum tributary concentration distributions using the Mann-Whitney Rank Sum test. Values reported are the P-value from the test. If P-value is less than the significance level ( $\alpha = 0.05$ ) a statistically significant difference in median values is present, otherwise the medians are not statistically different. Classification of 'significantly greater' or 'significantly less' is based on the main-stem relative to the tributary.

	MS-1 (n = 411)	MS-2 (n = 492)	MS-3 (n = 458)
T-2 – high (n = 416)	<i>Nitrate</i> P < .001 (significantly less)	P < .001 (significantly less)	P = .573 (not differentiable)
T-3 – low (n = 434)	P = .294 (not differentiable)	P < .001 (significantly greater)	P < .001 (significantly greater)
T-2 – high (n = 416)	<i>Phosphate</i> P < .001 (significantly less)	P < .001 (significantly less)	P < .001 (significantly greater)
T-3 – low (n = 434)	P < .001 (significantly greater)	P < .001 (significantly greater)	P < .001 (significantly greater)
T-2 – high (n = 416)	<i>Total Nitrogen</i> P < .001 (significantly less)	P < .001 (significantly less)	P = .270 (not differentiable)
T-1 – low (n = 456)	P = .142 (not differentiable)	P < .001 (significantly greater)	P < .001 (significantly greater)
T-2 – high (n = 416)	<i>Total Phosphorus</i> P < .001 (significantly less)	P < .001 (significantly less)	P < .001 (significantly greater)
T-1 – low (n = 456)	P < .029 (significantly greater)	P < .001 (significantly greater)	P < .001 (significantly greater)

**Table 3**

Frequency (years) of statistically significant intrinsic mode functions from the empirical mode decomposition analysis of tributary and main-stem sites.

Parameter	T-1	T-2	T-3	T-4	MS-1	MS-2	MS-3
Flow Depth	0.69	0.61	0.25	0.74	1.00	0.48	0.83
	1.18	0.95	0.42	1.33	2.22	0.95	1.43
	2.86	1.67	0.87	2.50		1.33	2.50
	5.00	2.22	1.54	5.00			4.00
		3.33	2.50				
		5.00	4.00				
			6.67				
Nitrate	1.05	0.80		0.95	4.0	0.34	0.47
	2.00	6.67		2.50		0.80	0.91
	3.33					1.25	1.54
	3.33						
Total Nitrogen	0.49	0.61	0.63	0.63	0.80	0.43	0.87
	0.83	0.91	0.91	1.18		1.18	1.43
	1.54	1.43	1.67	2.50		1.54	2.86
		2.22	2.22			5.00	
		6.67					
Phosphate	0.87	1.18	1.82	0.61	1.00	0.95	0.71
	1.05	3.33	3.33	1.18	2.22	2.22	1.05
	1.82	5.00	5.00	1.67	6.67	6.67	2.00
	3.33			2.86			2.86
	6.67			6.67			5.00
Total Phosphorus	0.65	3.33	0.65	0.42	0.74	0.95	0.53
	0.95		1.00	0.91	1.82	2.86	0.87
	2.50		1.67	1.67	6.67		1.43
	4.00		3.33	3.33			2.22
			5.00				

**Fig. 3.** Time series of significant intrinsic mode functions (IMFs) from the Empirical Mode Decomposition analysis for  $\text{NO}_3$  (left) and TN (right) concentrations at UBWC monitoring sites. TS1 and MS 1 are at the top. Note: x-axis label reflects Month-Year.

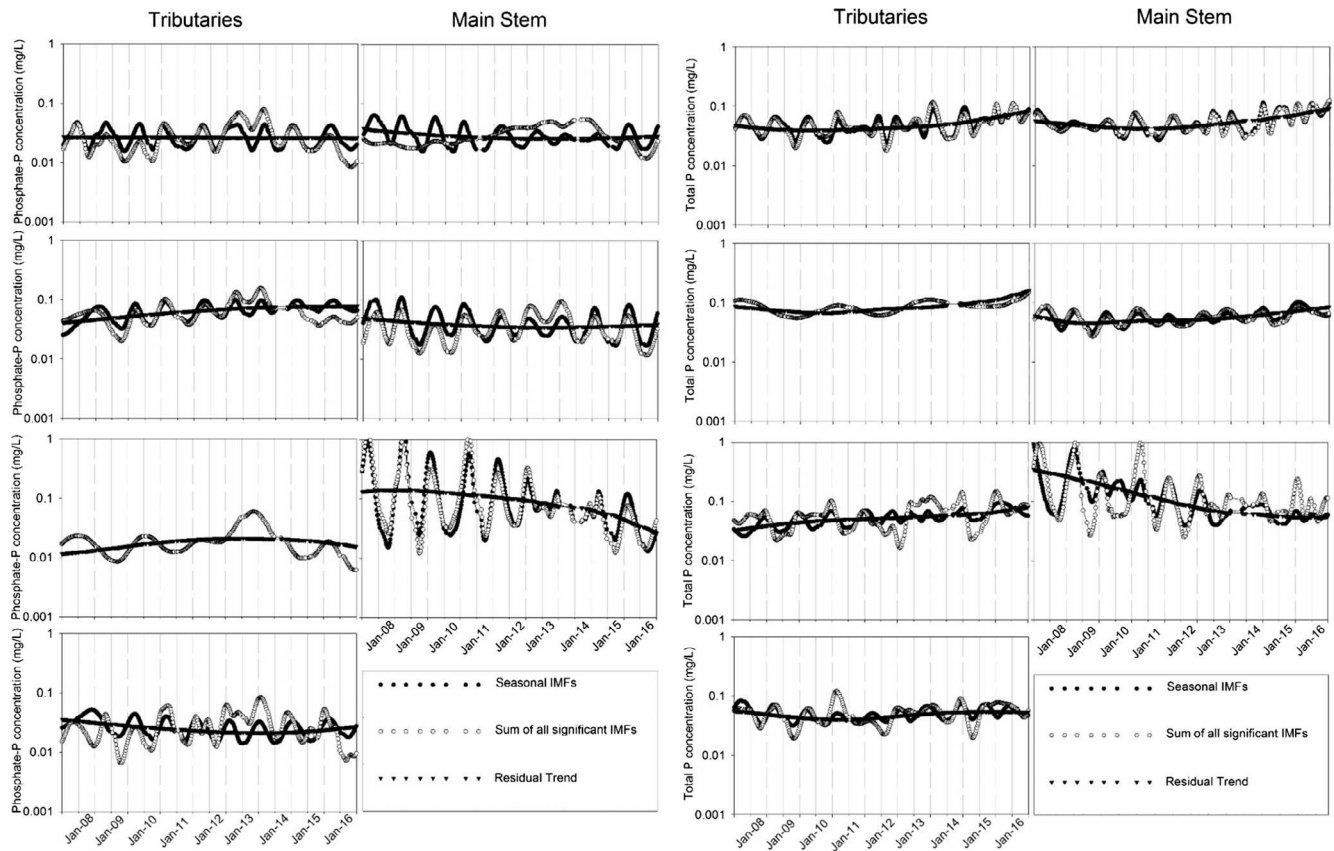


**Fig. 4.** Time series of significant intrinsic mode functions (IMFs) from the Empirical Mode Decomposition analysis for  $\text{PO}_4$  (left) and TP (right) concentrations at UBWC monitoring sites. TS1 and MS 1 are at the top. Note: x-axis label reflects Month-Year.

monitored tributaries (Fig. 5). Regarding  $\text{NO}_3\text{-N}$ , no statistically significant seasonal trend was observed for MS-1; however, MS-2 generally fell within the range observed for tributary seasonal trends. Nevertheless, we found minimum concentrations to fall on the high side of the tributary seasonal trend range. For DRP, we found MS-1 to fall on the lower side of the tributary seasonal trend range year-round, while MS-2 fell on the higher side of the tributary seasonal trend range in summer and low-side of the range in winter and spring. It is important to note the unique deviation of MS-3 from the results of all other study sites. Results in Fig. 5 highlight a long-term residual decrease in all nutrient time-series. Preceding January 2013, all parameters showed distinct downward trends that level out, or increase thereafter. Trends for N at MS-3 were not significantly different from results found at T-2 (Table 2); however, the timing of  $\text{NO}_3\text{-N}$  peaks and valleys prior to 2014 was more reflective of P dynamics with peaks in summer and valleys in winter (Fig. 5). Regarding P, the timing of DRP and TP concentrations in MS-3 were the same as results found for other tributaries and main-stem sites, with the main difference being the amplitude of the trends, especially pre-2014. Trend concentration gradients of both DRP and TP for MS-3 were an order of magnitude greater than trends found for other sites in the UBWC (0–2.0 mg/L instead of 0–0.4 mg/L).

### 3.3. Comparison with descriptive variables

Scatterplots and linear regressions were performed to determine how flow and water quality parameters were related to nutrient concentrations. Simple linear regressions of noise-defined herein as the raw data minus the sum of statistically significant IMFs showed a positive correlation between flow rate and nutrient

concentrations for all parameters (Table 4a). Coefficients of determination varied widely among sites and water quality parameters (0.01–0.33). The positive relationship between noise of flow and nutrient parameters likely reflects surface runoff during storm events that dissolve and entrain fertilizers and P rich surface soils via surface and subsurface macropore pathways, which is well recognized to occur in the studied landscape (Ford et al., 2015a; Williams et al., 2016). Linear regressions between statistically significant seasonal trends for flow rate and nutrient concentrations highlight contrasting dynamics for N and P species (Table 4b). Regarding baseflow seasonal trends in N species, both  $\text{NO}_3\text{-N}$  and TN relationships were positively correlated for all sites except for MS-3 in which a near zero slope was observed. Conversely, P showed an inverse relationship (decreased concentrations with increased flow) for all sites except for TP from T-3. As previously mentioned, T-3 did not have statistically significant seasonal trends for DRP, but did for TP, which was reminiscent of N seasonality. Total P had less distinct inverse relationships with flow compared to DRP. For instance, at T-2 there was no distinct seasonal trend for TP and there was a negative relationship for DRP. Similarly, at MS-2, the slope for TP was nearly equal to zero.

To further investigate factors impacting the contrasting findings for DRP and  $\text{NO}_3\text{-N}$  dynamics, qualitative comparison of statistically significant trends for MS-2 was performed with pH, DO, and temperature measured at a nearby USGS gauging station (Fig. 6). Descriptions are qualitative since the USGS data was an incomplete time series that did not include data in the winter (and hence EMD could not be performed). Peak DRP concentration in the summer closely aligned with maximum values of temperature, minimum values of DO, and minimum values of pH. Nitrate was inversely related to temperature and tightly linked to DO concentration.

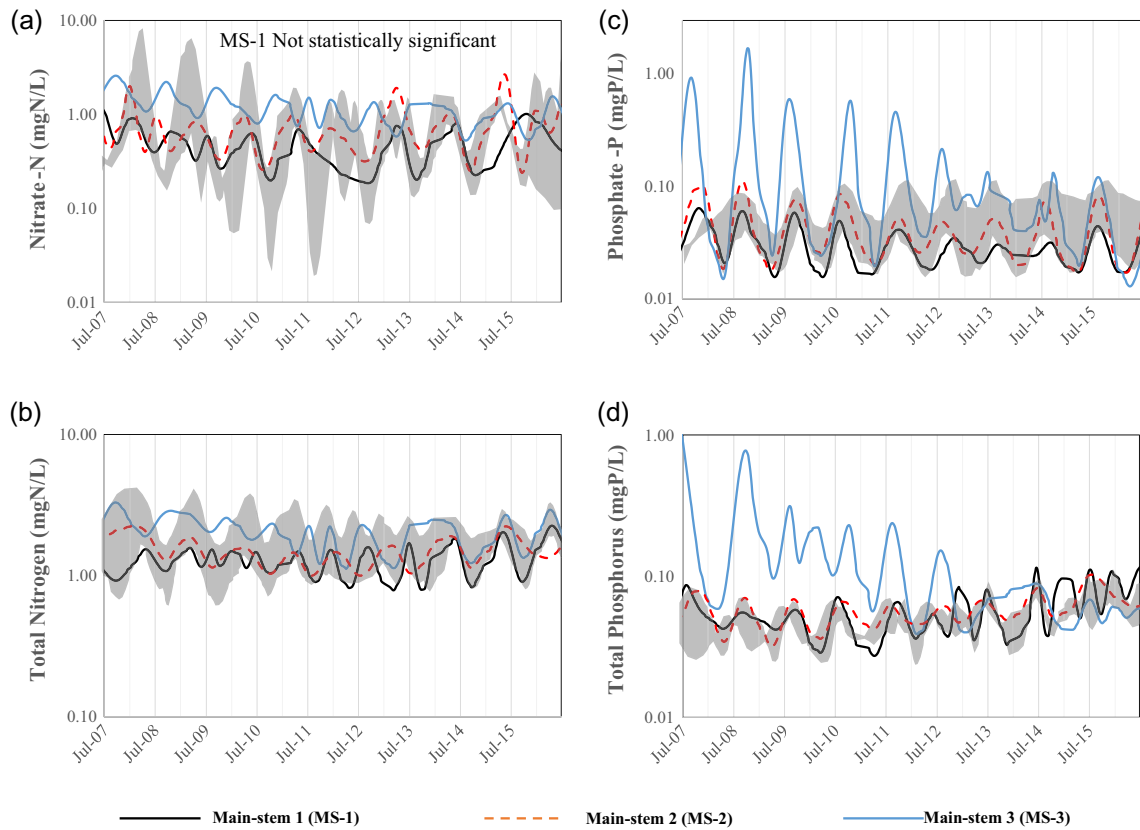


**Fig. 5.** Dissolved nutrient comparison for (a) nitrate, (b) total nitrogen, (c) phosphate, and (d) total phosphorus for statistically significant seasonal fluctuations (added to baseline trend) for main-stem sites with the range of statistically significant trends (noted by the shaded region) for tributary sites. Note: x-axis label reflects Month-Year.

**Table 4**

Results of the linear regression analysis for (a) noise, and (b) statistically significant seasonal IMFs. Regressions follow the form of  $y = m^*x + b$ , where  $y$  represents nutrient concentration,  $m$  represents the slope coefficient,  $x$  represents flow depth, and  $b$  reflects the  $y$ -intercept (assumed zero). The slope ( $m$ ) and coefficient of determination ( $R^2$ ) are reported.

a) Noise	"y"	T-1	T-2	T-3	T-4	MS-1	MS-2	MS-3
Slope of linear regression (m)	NO3	1.13	1	1.86	1.04	2.09	1.23	0.55
	PO4	0.84	1.51	0.93	0.81	0.76	1.14	0.3
	TN	0.56	0.78	0.56	0.62	1.1	0.85	0.5
	TP	0.75	1.36	0.68	0.77	0.92	1.09	0.42
Coefficient of determination ( $R^2$ )	NO3	0.02	0.01	0.01	0.05	0.08	0.16	0.03
	PO4	0.13	0.19	0.03	0.16	0.06	0.25	0.01
	TN	0.1	0.07	0.04	0.14	0.19	0.21	0.05
	TP	0.15	0.2	0.04	0.19	0.13	0.33	0.04
b) Seasonal IMFs		T-1	T-2	T-3	T-4	MS-1	MS-2	MS-3
Slope of linear regression (m)	NO3	3.64	1.71	N/A	1.01	N/A	1.21	-0.06
	PO4	-1.04	-0.26	N/A	-0.59	-1.03	-0.72	-3.09
	TN	0.88	0.41	0.46	0.22	0.43	0.29	-0.09
	TP	-0.3	N/A	0.2	-0.31	-0.34	-0.03	-1.14
Coefficient of determination ( $R^2$ )	NO3	0.18	0.08	N/A	0.19	N/A	0.25	0
	PO4	0.12	0.01	N/A	0.28	0.46	0.1	0.29
	TN	0.14	0.07	0.4	0.09	0.21	0.12	0
	TP	0.01	N/A	0.27	0.16	0.09	0	0.06

\* N/A denotes absence of statistically significant IMF for either flow or nutrient time-series analysis.

We also provide qualitative comparison of the MS-2 site with a small monitored watershed ( $4 \text{ km}^2$ ) with extensive tile drainage and a monitored tile main ( $2 \text{ km}^2$ ) from 2005 to 2012 (Figs. 7 and 8). This data has been previously published elsewhere (King et al., 2014b). Results for the small watershed and tile main generally mimicked findings from MS-2 (Fig. 7). For both the tile main and small watershed, peak N dynamics occurred in the first half

of the year (Jan–June) while peak P dynamics occurred in the second half of the year (July–December). Of note, tile drain N concentrations in the summer and fall months were consistently greater than that of the small watershed, while concentrations were equivalent in winter and spring. For P, no distinct visual differences were observed between tile drains, the small watershed and seasonal trends at MS-2.

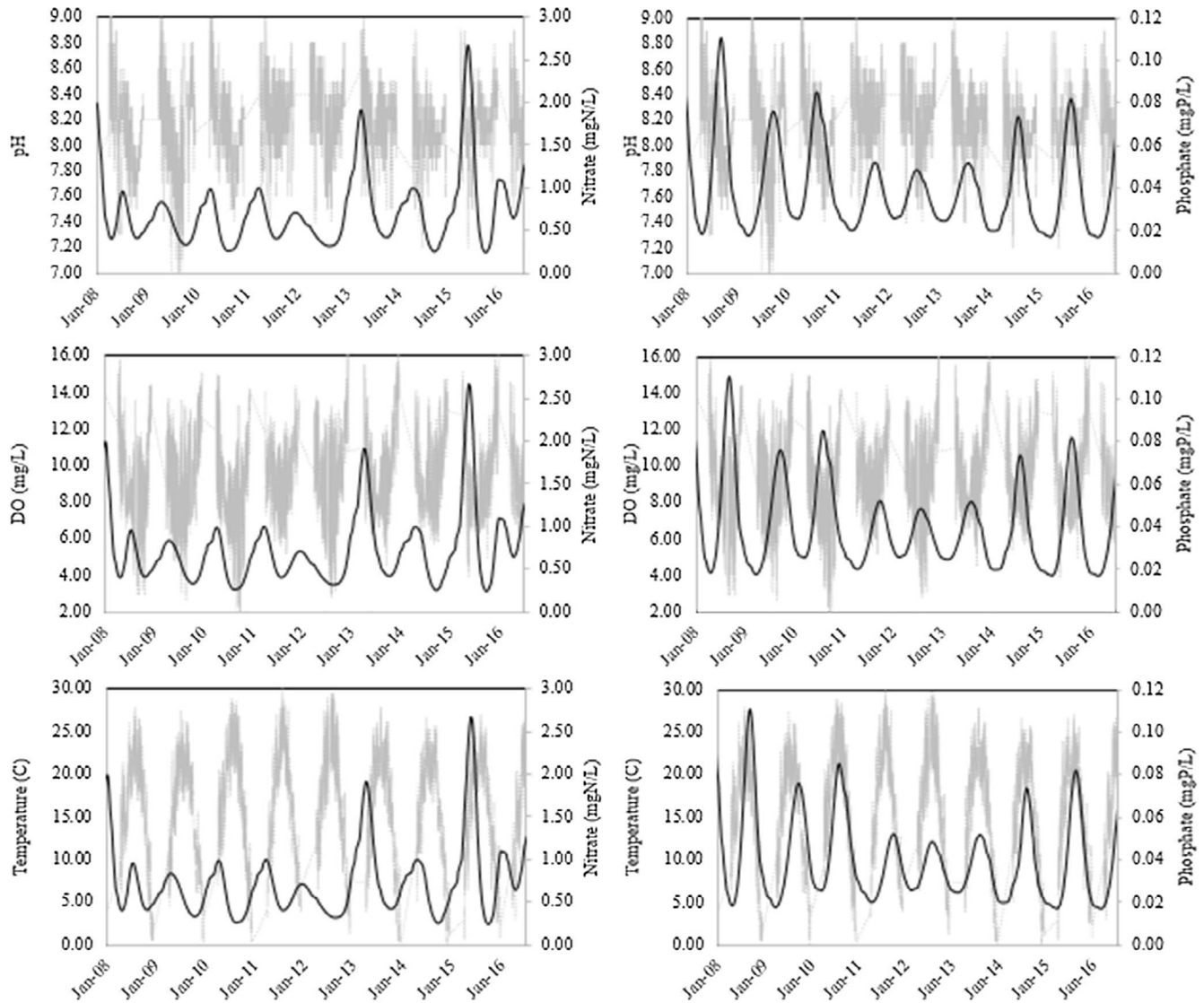


**Fig. 6.** Time-series comparison of seasonal trends for dissolved nutrient concentrations at MS-2 with pH, dissolved oxygen, and temperature at USGS gauging station 03228300 from 2008 to 2016. Water quality data from the USGS station were not available during winter, hence EMD analysis could not be conducted on the time series. Note: x-axis label reflects Month-Year.

To better understand sources of baseflow fluctuations, the relationship between dissolved and total nutrient concentration for the small watershed and tile main was investigated (Fig. 8). Regarding P dynamics, we found that TP dynamics were governed primarily by DRP in tile drains year-round as evidenced by a slope close to one (1.2) and a high  $R^2$  of 0.67 for the linear regression. For the small watershed, we found that the high DRP concentrations (reflecting seasonal peaks in dry summer conditions) governed TP dynamics. However, we found an inverse relationship between DRP and TP for low DRP conditions (e.g., <0.1 mg P/L) which coincide with wetter antecedent moisture conditions in winter and spring. This finding was evidenced by a higher slope from the linear regression (1.67) and poor  $R^2$  value (0.09), highlighting the non-linearity of the TP-DRP relationship at the small watershed scale. The increase in TP during high baseflow conditions in winter and spring are reflective of the decreased slope of flow-TP relationships for seasonal fluctuations (Table 4). Similar to tile P dynamics, we found that both the tile and small watershed site showed tight correlation between  $\text{NO}_3\text{-N}$  and TN (slopes of 1.18 and 1.21 respectively with  $R^2$  values of 0.91 and 0.80 respectively) highlighting the significance of  $\text{NO}_3\text{-N}$  for downstream N loading. For these reasons,

we do not place further emphasis on TN in the discussion to avoid redundancy with  $\text{NO}_3\text{-N}$  discussion.

## 4. Discussion

### 4.1. Upland and in-stream controls on baseflow nutrient concentrations

#### 4.1.1. Phosphorus

Results of the time-series analysis for tributary and main-stem sites suggest that upland soil drainage exerts a strong control on the timing of baseflow DRP concentrations. Peak concentrations of DRP in summer followed by minimum DRP in late-winter to early-spring in both tributaries and main-stem sites were reflective of seasonal trends observed from the tile drain and the small 4 km<sup>2</sup> watershed in which concentration was inversely related to baseflow flow depth (Figs. 4, 5c–d, Table 4). During the winter and early spring when antecedent moisture is high and water residence times in the soil are low, leaching of surface fertilizers and soil P to tile drains is well recognized, especially following storm events (Williams et al., 2016). However, during the summer it is unlikely

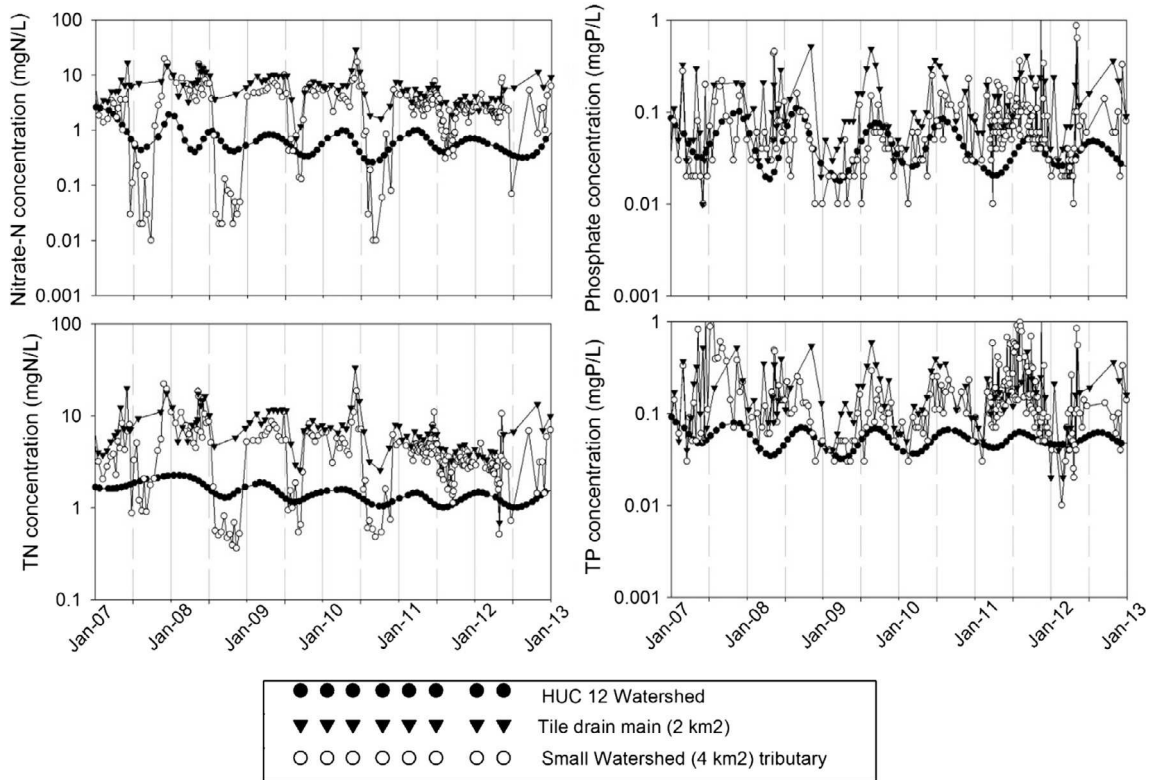


**Fig. 7.** Time-series showing statistically significant seasonal oscillations (base-flow trends) for MS-2, and raw datasets for the 2 km<sup>2</sup> tile drain and the 4 km<sup>2</sup> watershed tributary. EMD was not performed on the small watershed data due to inconsistencies in data collection frequency. Note: x-axis label reflects Month-Year.

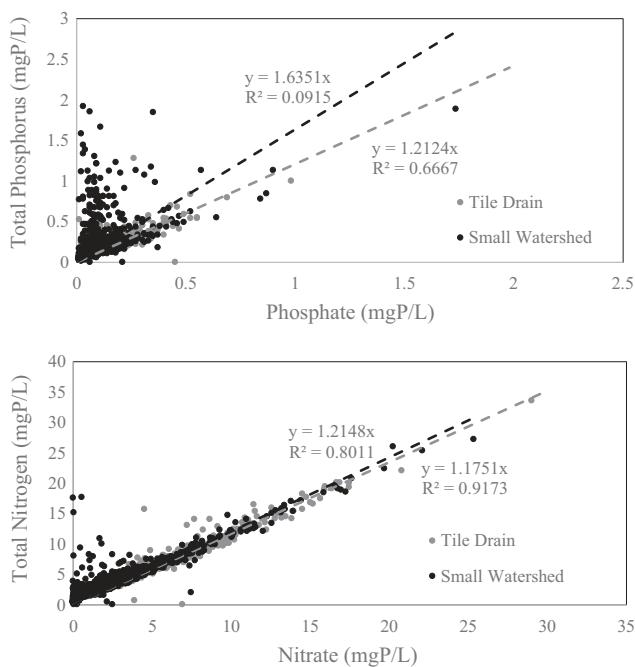


**Fig. 8.** Linear regression between measured dissolved and total nutrient concentrations for (a) phosphorus and (b) nitrogen for the small watershed (4 km<sup>2</sup>) and tile drain (2 km<sup>2</sup>) located within the UBWC (see Fig. 1 for location).

that leaching from high soil-test P soils or fertilizers at the surface governs baseflow concentrations given the dis-connectivity of the tile-drains and the seasonal water table. Tile drains provide a small proportion of flow in the summer and, as a result, subsurface leaching of P following storm events is subjected to more tortuous

percolation through a deeper saturated aquifer before resurfacing to stream channels (Exner-Kittridge et al., 2016). Soil bound inorganic P in agricultural landscapes is also often highly stratified (Ford et al., 2015a); thus, we would not suspect desorption of inorganic P from soils in deeper aquifers to support high concentration of DRP during the summer. If this were the case, we would have expected to see higher concentrations in winter. We therefore hypothesize that high baseflow DRP concentrations during warm summer months reflect re-mineralization of organic P in the soil column and subsequent delivery to the stream channel through subsurface pathways below the tile drains, while leaching of inorganic P from surface soils or lower rates of re-mineralization (due to decreased microbial activity) and subsequently delivery through tile drains controlled concentrations during the winter months.

Results from the current study adds to a growing body of literature that suggests organic matter mineralization is an important pathway in fluvial P cycling and merits enhanced research efforts. A recent edge-of-field modeling study of the Agricultural Policy Environmental Extender (APEX) model supports the concept of mineralization of organic matter to control baseflow concentration in central and northwestern Ohio tile-drained landscapes (Ford et al., 2015a). Ford et al., (2015a) highlights the potential of mineralization of organic rich soils to support baseline DRP concentrations exceeding eutrophic standards (Dodds et al., 1998; King et al., 2014a). As a second example, Joshi et al. (2015) recently used a novel phosphate isotope fingerprinting approach to identify re-mineralization of inorganic P from organic sediment as a predominant source within the Chesapeake Bay. Utilizing fingerprinting methods and numerical models that are sensitive to such processes are key areas for future research to build towards comprehensive watershed P budgets and development of appropriate upland management strategies.

While time series analyses suggest that upland soil drainage was important for determining the timing of baseflow DRP concen-

tration, results of longitudinal gradients along the main-stem highlight the importance of in-stream processes to control peak DRP concentrations in the summer. Longitudinal results showed an increase of DRP in summer-fall months between MS-1 and MS-2, but relatively stable DRP concentrations in winter-spring months. The increases in summer DRP concentration could either reflect additional upland source contributions from the additional 59 km<sup>2</sup> drainage area (Table 1), or it could be a result of an in-stream source due to changing water quality conditions. We marginalize the likelihood of the potential for an additional upland source through a simple mass-balance calculation assuming drainage area proportional flow rates in 2008. Given that MS-1 statistically significant seasonal trends were found to be 0.059 mg P/L and that its drainage area represented 77% of the drainage area at MS-2 (where the seasonally high concentration was 0.10 mg P/L for 2008), we calculated that concentrations from the additional drainage area at MS-2 would need to be 0.23 mg P/L, which is nearly double that of seasonably high DRP concentrations observed in the small watershed (Fig. 7) and the statistically significant seasonal trends in the highest DRP tributary (Fig. 4). Based on these findings, our results suggest that upland processes exert strong control on DRP concentrations in the winter and spring months, while coupled upland and in-stream conditions control watershed baseflow DRP concentrations during summer and early fall.

Regarding processes, our results suggest that in-stream increases of DRP to the stream channel under low-flow summer conditions is likely reflective of favorable water quality conditions for DRP release from benthic sediments. While organic matter mineralization of benthic sediments is a possible source of increased DRP, we suspect this is low given the lack of sensitivity of other dissolved nutrient concentrations to sediment organic matter mineralization rates in agricultural streams, i.e., dissolved inorganic carbon (Ford and Fox, 2014; Ford and Fox, 2015) and NO<sub>3</sub>-N (Ford et al., 2017a). However, recent studies have highlighted the ability of microbial activity in benthic biofilms by polyphosphate accumulating organisms to enhance DRP release in streams (Saia et al., 2017). Under low-oxygen, warm summer months (Fig. 6) it is plausible that microbial biota release labile inorganic P through this mechanism. Increased DRP concentration may also reflect favorable water quality conditions for DRP desorption and dissolution from inorganic P stores within benthic sediments. Results from the current study show tight linkages between maximum DRP concentrations and seasonally elevated temperature, and seasonally low pH and dissolved oxygen levels (Fig. 6). Several previous studies have highlighted the release of DRP to stream and lake water under anaerobic, low pH conditions due to desorption from sediment surfaces and dissolution of phosphate precipitates due to favorable redox conditions for iron-bound P (Wang et al., 2008; Wu et al., 2014). Further work is needed to tease out the controlling mechanism in laboratory incubations, or through novel tracer approaches, such as PO<sub>4</sub>-oxygen isotopes. Further discussion is presented in Section 4.2.

Results of the time-series analysis for total nutrient concentrations in tributary and main-stem sites showed that TP dynamics deviated from DRP at high baseflow due to in-stream particulate P erosion and transport. Time-series analysis results for TP highlight the importance of particulate P contributions in winter and spring when baseflow is high and DRP contributions are low (Figs. 4, 5, and 8). The less pronounced inverse relationship, and sometimes shift to positive relationship, of TP with flow as compared to DRP (Table 4) reflects tile drainage water that enters the channel with low sediment concentrations. This mechanism is further supported by the tight correlation between DRP and TP for tile and the poor correlation for DRP and TP in the small watershed (Fig. 7). It is well recognized that the stream channel will scour loosely deposited sediments from the streambed to fulfill the sed-

iment transport carrying capacity, even in low-flow conditions (Russo and Fox, 2012; Ford and Fox, 2014). Streambed sediments will partially reflect erosion from upland soils which, as we have previously mentioned, are rich in soil test P in the region (King et al., 2014a; Ford et al., 2015a,b).

#### 4.1.2. Nitrate

Similar to DRP results, statistically significant seasonal trends of NO<sub>3</sub>-N in tributary and main-stem sites suggest upland controls governing concentrations in winter and spring. Regarding source water contributions, shallow subsurface water is typically enriched in NO<sub>3</sub>-N relative to groundwater (Exner-Kittridge et al., 2016). For winter and spring baseflow, this theory describes our results given that the most intensely drained tributaries (Tributaries 1 and 2) had the highest winter/spring NO<sub>3</sub>-N concentrations and the least intensively drained tributary (Tributary 4) had the lowest peak NO<sub>3</sub>-N concentrations. For main-stem sites, MS-2 has slightly greater peak values as compared to MS-1, which could be attributed to the increased drainage density for the additional drainage area between MS-1 and MS-2 (see Table 1). These results point to the potential for tile drainage to enhance baseline NO<sub>3</sub>-N levels when the vadose-zone has higher antecedent moisture.

Results for seasonally low NO<sub>3</sub>-N concentrations during low antecedent moisture reflect a mixture of upland and in-stream controls. Tile drains contribute a small proportion of flow during the dry summer months and hence, source water contributions depleted in NO<sub>3</sub>-N were expected and occurred in all tributary and main-stem sites (reflective of the small watershed results). We hypothesized that as the watershed size increased, connectivity with the deeper aquifers and in-stream biological processing would increase and, as a result, NO<sub>3</sub>-N concentrations at main stem sites would decrease relative to upstream tributaries. The assertion of in-stream biotic processing during warm summer months is reasonable given the high stream water temperature and low dissolved oxygen levels measured at MS-2 (Fig. 6) that promote favorable water quality conditions for autochthonous growth and denitrification (Mulholland et al., 2008; Griffiths et al., 2012; Ford et al., 2017a). Our results contradict this hypothesis since main-stem sites (downstream of the tributary) have seasonally low concentrations that are >0.1 mg N/L. Recent studies in agroecosystem streams have shown that denitrification and algal NO<sub>3</sub>-N uptake can be on the same order of magnitude and that the potential downstream fate of the regenerated N from transient storage and algal biomass could become important (Hotchkiss and Hall, 2015; Webster et al., 2016; Ford et al., 2017a). Our finding provides evidence that this regenerative fate of algal N may fuel downstream N increases which has significant implications for downstream reservoirs and waterbodies subjected to harmful and nuisance algal blooms. Explicitly accounting for N fate, transport, and exchange in these various pools in watershed-scale models will be critical for quantifying flux pathways and nutrient management at varying watershed-scales.

#### 4.1.3. Sensitivity of seasonal nutrient concentrations to disturbance near the outlet

Time-series analysis results for MS-3, the last main-stem site before the Hoover reservoir, were unique relative to the other tributary and main-stem sites within the UBWC watershed. We found disequilibrium conditions from fall 2006 through 2013 for all water quality parameters that subsequently returned to equilibrium. We hypothesize that this finding was reflective of small perturbations near the watershed outlet. Our findings showed significantly higher DRP and NO<sub>3</sub>-N concentrations that were not differentiable from high tributary nutrient distributions (Fig. 2; Table 2). MS-3 drains an additional 22 km<sup>2</sup> (<10% of the total drainage area) over MS-2, but shows NO<sub>3</sub>-N concentrations that are

twofold greater and DRP concentrations that are 10-fold greater during seasonally high periods (Figs. 3 and 4). Upon visual inspection of aerial photographs during this timeframe the only notable change was associated with a small development upstream of MS-3 within the additional drainage area. Based on photographs from 2005, 2009, 2011, 2014, and 2016, it appears that the development started in 2005 and was completed by 2014. The impact of conversion of agricultural land for urban and suburban land use is well known to increase sediment delivery to stream channels, and the authors postulate that high sediment loads (especially early in the disturbance) were deposited to the stream adjacent to the construction site and were subsequently subjected to microbial mineralization and DRP release during low-flow, warm summer months.

Seasonal timing of peaks and valleys and differences in magnitudes between  $\text{NO}_3\text{-N}$  and DRP concentrations support the hypothesis of sediment deposits to fuel disequilibrium conditions at MS-3 from 2006 and 2013. Statistically significant  $\text{NO}_3\text{-N}$  concentrations during the disturbance shifted to being high in summer and fall and low in winter (analogous to watershed DRP dynamics), and then reversed post-disturbance. However, we note that concentrations of  $\text{NO}_3\text{-N}$  during winter and spring were comparable to MS-2. This would suggest a pulse of  $\text{NO}_3\text{-N}$  occurring in warm summer months. We would not suspect this to be tied to upland processes given the dis-connectivity between tile drains and the stream channel during warm (low antecedent moisture) summer months and the return to equilibrium processes in later years. Given the occurrence in summer, this is likely attributed to benthic microbial ammonification and nitrification, resulting in  $\text{NO}_3\text{-N}$  regeneration to the stream channel. Further, the 10-fold magnitude increase in DRP concentrations during summer months reflects rapid desorption or release of P by polyphosphate accumulating biofilms acting on labile P in streambed sediments. Polyphosphate accumulating organisms are commonly used as an enhanced biological P removal platform in wastewater facilities; however, they release P under anaerobic conditions (Saia et al., 2017). Proliferation of microbial communities in this stream reach are likely enhanced by the small wastewater facility discharges both upstream and downstream of the urbanizing disturbance (Fig. 1). While at a different spatial scale, our results are reminiscent of findings from a large-scale SPARROW model of the Mississippi River Basin (Alexander et al., 2008) that highlight the importance of managing nutrient dynamics near large rivers (or fast flowing streams) to achieve load and concentration reductions at the environmentally relevant scale. Specifically, our result highlights the importance of minimizing nutrient-rich sediment pulses to stream channels that then settle out and are subjected to biotic and abiotic processes near receiving waterbodies.

#### 4.2. Broader implications for tile-drained agroecosystems

Results of the study for baseline P concentrations in tile-drained agroecosystems show non-rate limiting conditions of algal proliferation, suggesting alternative mechanisms may be needed for managing DRP baseline flows. Our findings of watershed baseflow DRP concentrations are significant given that watershed scale bioavailable DRP concentrations at MS-2 oscillated between an average minimum and maximum seasonal concentration of 0.02 and 0.08 mg P/L, respectively (Fig. 5). Eutrophic conditions in freshwater lakes are established above TP thresholds of 0.071 mg P/L (Dodds et al., 1998). However, it is well recognized that DRP concentrations exceeding 0.03 mg P/L create conditions conducive to algal proliferation (King et al., 2014a). While much emphasis has been placed on managing DRP through effective field BMPs and agronomic practices to reduce runoff from surface applied fertilizers and leaching from high soil test P soils, broadly they have resulted in insufficient water quality improvements (Shapley

et al., 2013, 2015). Our results of baseflow DRP to favor more chronic legacy phosphorus issues, high organic matter turnover in soils, and benthic sediment release partially highlight why such BMPs have led to insufficient improvements, especially in systems with low residence times. The implication is that more systematic in-stream management strategies may need to be coupled with upland management to mitigate environmentally harmful concentration thresholds. We note the challenge that results of this study presents, given that mechanisms have contrasting impacts on nutrient regeneration/attenuation. We caution that practitioners be cognizant of the potential unintended consequences of promoting conditions such as anaerobic zones for denitrification.

While  $\text{NO}_3\text{-N}$  levels at baseflow are generally below eutrophic levels during summer and fall, the elevated baseline  $\text{NO}_3\text{-N}$  levels in winter and spring originating from tile drains make receiving surface water bodies susceptible to drinking water contamination. In the UBWC watershed, the Hoover reservoir is susceptible to excess  $\text{NO}_3\text{-N}$  levels exceeding 10 mg/L, which makes the water toxic for infants due to the transformation of hemoglobin to methemoglobin, which has limited oxygen carrying capacity. In recent years,  $\text{NO}_3\text{-N}$  levels were well above the EPA thresholds in the reservoir, which serves as the drinking water source for nearly 8,000,000 residents in and around the city of Columbus, OH. While we did not find statistically significant seasonal pulses to exceed this threshold, our results show baseline levels at MS-2 upwards of 3 mg N/L. Therefore, the reservoir may become more sensitive (i.e., have less buffering capacity) to pulses of N in stormflow that result in exceedance of the 10 mg N/L threshold. A potential mitigation strategy to reducing  $\text{NO}_3\text{-N}$  levels during environmentally sensitive periods is inclusion of drainage water management systems in intensively drained areas. Drainage water management has been found to significantly reduce  $\text{NO}_3\text{-N}$  loading in a nearby watershed by reducing tile discharge, i.e., holding the water in the field (Williams et al., 2015b). While Williams et al. (2015b) found that  $\text{NO}_3\text{-N}$  concentrations in drainage water were not statistically different pre-and post-drainage water management, the reduction in water flux allows deeper percolation and mixing with subsurface water, therefore a smaller proportion of baseflow is associated with tile drainage. Findings from our study suggest that lower intensity tile-drained watersheds have lower seasonally high concentrations in winter and spring, therefore widespread implementation could provide significant reductions in reservoir  $\text{NO}_3\text{-N}$  concentrations during this timeframe.

## 5. Conclusions

Collectively, our study highlights the importance of both in-stream and upland controls on nutrient baseflow concentrations in tile-drained agricultural landscapes. Further work is needed at the watershed scale to model and quantify the extent of these identified controls. Specifically, our results support the potential importance of upland management strategies, e.g., drainage water management, and within-channel mitigation to alter nutrient concentration dynamics at baseflow conditions. Given the contrasting dynamics of N and P, caution should be taken when promoting specific practices, as it may promote unintended consequences, e.g., DRP release in anoxic zones that promote denitrification. Sustainable solutions will be especially important to combat increasing prominence of algal blooms that occur in rivers and small reservoirs with low residence times where baseflow nutrient concentrations fuel ecosystem dynamics.

## Acknowledgements

The authors would like to thank Eric Fischer for analytical expertise; and Jedediah Stinner, Katie Rumora, and especially

Marie Pollock, for help in data collection and analysis. We also thank the two anonymous reviewers whose comments significantly improved the quality of the manuscript. This is publication No. 17-05-039 of the Kentucky Agricultural Experiment Station and is published with the approval of the Director. This work is supported by the National Institute of Food and Agriculture, U.S. Department of Agriculture.

## References

Alexander, R.B., Smith, R.A., Schwarz, G.E., Boyer, E.W., Nolan, J.V., Brakebill, J.W., 2008. Differences in phosphorus and nitrogen delivery to the Gulf of Mexico from the Mississippi River Basin. *Environ. Sci. Technol.* 42, 822–830.

Arnold, J.G., Harmel, R.D., Johnson, M.V., Bingner, R., Strickland, T.C., Walbridge, M., Santhi, C., DiLuzio, M., Wang, X., 2014. Impact of the Agricultural Research Service watershed assessment studies on the conservation effects assessment project cropland national assessment. *J. Soil Water Conserv.* 69 (5), 137A–144A.

Baker, D.B., Johnson, L.T., Confesor, R.B., 2017. Vertical stratification of soil phosphorus as a concern for dissolved phosphorus runoff in the Lake Erie Basin (J. Environ. Qual. in press).

Blann, K.L., Anderson, J.L., Sands, G.R., Vondracek, B., 2009. Effects of agricultural drainage on aquatic ecosystems: a review. *Crit. Rev. Environ. Sci. Technol.* 39, 909–1001. <https://doi.org/10.1080/10643380801977966>.

Christianson, L.E., Harmel, R.D., Smith, D., Williams, M.R., King, K., 2016. Assessment and synthesis of 50 years of published drainage phosphorus losses. *J. Environ. Qual.* 45, 1467–1477.

Dodds, W.K., Jones, J.R., Welch, E.B., 1998. Suggested classification for stream trophic state: distributions of temperate stream types by chlorophyll, total nitrogen, and phosphorus. *Wat. Res.* 32 (5), 1455–1462.

Exner-Kittridge, M., Strauss, P., Bloschl, G., Eder, A., Saracevic, E., Zessner, M., 2016. The seasonal dynamics of the stream sources and input flow paths of water and nitrogen of an Austrian headwater agricultural catchment. *Sci. Total Environ.* 542, 935–935.

Ford, W.I., Fox, J.F., 2014. Model of particulate organic carbon transport in an agriculturally impacted stream. *Hydrol. Process.* 28 (3), 662–675.

Ford, W.I., Fox, J.F., 2015. Isotope based Fluvial Organic Carbon (ISOFLOC) model: model formulation, sensitivity and evaluation. *Wat. Resour. Res.* 51 (6), 4046–4064.

Ford, W.I., King, K.W., Williams, M.R., Williams, J., Fausey, N.R., 2015a. Sensitivity of the Agricultural Policy/Environmental eXtender (APEX) for phosphorus loads in tile-drained landscapes. *J. Environ. Qual.* 44, 1099–1110.

Ford, W.I., Fox, J.F., Pollock, E., Rowe, H., Chakraborty, S., 2015b. Testing assumptions for nitrogen transformation in a low-gradient agricultural stream. *J. Hydrol.* 527, 908–922. <https://doi.org/10.1016/j.jhydrol.2015.05.062>.

Ford, W., Fox, J., Pollock, E., 2017a. Reducing equifinality in an isotope-based stream nitrogen model highlights the flux of algal nitrogen from agricultural streams. *Wat. Resour. Res.* 53 (8), 6539–6561.

Ford, W., King, K., Williams, M., Confesor, R., 2017b. Modified APEX model for simulating macropore phosphorus contributions to tile drains. *J. Environ. Qual.* 46, 1413–1423.

Griffiths, N.A., Tank, J.L., Royer, T.V., Warner, T.J., Frauendorf, T.C., Rosi-Marshall, E.J., Whiles, M.R., 2012. Temporal variation in organic carbon spiraling in Midwestern agricultural streams. *Biogeochemistry* 108, 149–169.

Hartmann, A., Goldscheider, N., Wagener, T., Lange, J., Weiler, M., 2014. Karst water resources in a changing world: review of hydrological modeling approaches. *Rev. Geophys.* 52 (3), 218–242.

Hotchkiss, E., Hall, R.O., 2015. Whole-stream  $^{13}\text{C}$  tracer addition reveals distinct fates of newly fixed carbon. *Ecology* 96 (2), 403–416.

Huang, N.E., Shen, Z., Long, S.R., Wu, M.C., Shih, H.H., Zheng, Q., Yen, N., Tung, C.C., Liu, H.H., 1998. The empirical mode decomposition and the Hilbert spectrum for nonlinear and non-stationary time series analysis. *Proc. Math. Phys. Eng. Sci.* 454, 903–995.

Jarvie, H., Sharpley, A., Brahana, V., Simmons, T., Price, A., Neal, C., Lawlor, A., Sleep, D., Thacker, S., Haggard, B., 2014. Phosphorus retention and remobilization along hydrological pathways in karst terrain. *Environ. Sci. Technol.* 48 (9), 4860–4868.

Joshi, S.R., Kukkadapu, R.K., Burdige, D.J., Burden, M.E., Sparks, D.L., Jaisi, D.P., 2015. Organic matter remineralization predominates phosphorus cycling in the mid-bay sediments in the Chesapeake bay. *Environ. Sci. Technol.* 49 (10), 5887–5896.

King, K.W., Smiley Jr., P.C., Baker, B.J., Fausey, N.R., 2008. Validation of paired watersheds for assessing conservation practices in the Upper Big Walnut Creek watershed, Ohio. *J. Soil Water Conserv.* 63, 380–395.

King, K.W., Williams, M.R., Macrae, M.L., Fausey, N.R., Frankenberger, J., Smith, D.R., Kleinman, P.J.A., Brown, L.C., 2014a. Phosphorus transport in agricultural subsurface drainage: a review. *J. Environ. Qual.* <https://doi.org/10.2134/jeq2014.04.0163>.

King, K.W., Williams, M.R., Fausey, N.R., 2014b. Contributions of systematic tile drainage to watershed phosphorus transport. *J. Environ. Qual.* <https://doi.org/10.2134/jeq2014.04.0149>.

Koroleff, J., 1983. Determination of total phosphorus by alkaline persulfate oxidation. In: Grasshoff, K., Ehrhardt, M., Kremling, K. (Eds.), *Methods of Seawater Analysis*. Verlag Chemie, Wienheim, pp. 136–138.

Mulholland, P.J., Hill, W.R., 1997. Seasonal patterns in streamwater nutrient and dissolved organic carbon concentrations: separating catchment flow path and in-stream effects. *Wat. Resour. Res.* 33 (6), 1297–1306.

Mulholland, P., Helton, A., Poole, G., Hall, R., Hamilton, S., Peterson, B., Tank, J., Ashkenas, L., Cooper, L., Dahm, C., Dodds, W., Findlay, S., Gregory, S., Grimm, N., Johnson, S., McDowell, W., Meyer, J., Valett, H., Webster, J., Arango, C., Beaulieu, J., Bernot, M., Burgin, A., Crenshaw, C., Johnson, L., Niederlehrer, B., O'Brien, J., Potter, J., Sheibley, R., Sobota, D., Thomas, S., 2008. Stream denitrification across biomes and its response to anthropogenic nitrate loading. *Nature* 452, 202–206.

Peterson, B.J., Wollheim, W.M., Mulholland, P.J., Webster, J.R., Meyer, J.L., Tank, J.L., Martó, E., Bowden, W.B., Valett, H.M., Hershey, A.E., McDowell, W.H., Dodds, W.K., Hamilton, S.K., Gregory, S., Morrall, D.D., 2001. Control of nitrogen export from watersheds by headwater streams. *Science* 292 (5514), 86–90.

Pionke, H.B., Gburek, W.J., Schnabel, R.R., Sharpley, A.N., Elwinger, G.F., 1999. Seasonal flow, nutrient concentrations and loading patterns in stream flow draining an agricultural hill-land watershed. *J. Hydrol.* 220, 62–73.

Rato, R.T., Ortigueira, M.D., Batista, A.C., 2008. On the HHT, its problems, and some solutions. *Mech. Syst. Sig. Process.* 22, 1374–1394.

Richardson, C.W., Bucks, D.A., Sadler, E.J., 2008. The Conservation Effects Assessment Project benchmark watersheds: synthesis of preliminary findings. *J. Soil Water Conserv.* 63, 590–604.

Russo, J., Fox, J., 2012. The role of the surface fine-grained laminae in low-gradient streams: a model approach. *Geomorphology* 171, 127–138.

Saia, S.M., Sullivan, P., Regan, J.M., Carrick, H.J., Buda, A.R., Locke, N.A., Walter, M.T., 2017. Evidence of polyphosphate accumulating organism (PAO)-mediated phosphorus cycling in stream biofilms under alternating aerobic/anaerobic conditions. *Freshwater Sci.* (in press).

Shilling, K.E., Helmers, M., 2008. Tile drainage as karst: conduit flow and diffuse flow in a tile-drained watershed. *J. Hydrol.* 349, 291–301.

Schilling, K.E., Zhang, Y.K., 2004. Baseflow contribution to nitrate-nitrogen export from a large, agricultural watershed, USA. *J. Hydrol.* 295, 305–316.

Sharpley, A.N., Kleinman, P.J.A., Heathwaite, A.L., Gburek, W.J., Folmar, G.J., Schmidt, J.P., 2008. Phosphorus loss from an agricultural watershed as a function of storm size. *J. Environ. Qual.* 37, 362–368.

Sharpley, A., Jarvie, H., Buda, A., May, L., Spears, B., Kleinman, P., 2013. Phosphorus legacy: overcoming the effects of past management practices to mitigate future water quality impairment. *J. Environ. Qual.* 42, 1308–1326.

Sharpley, A., Bergstrom, L., Aronsson, H., Bechmann, M., Bolster, C., Borling, K., Djordic, F., Jarvie, H., Schoumans, O., Stamm, C., Tonderski, K., Ulen, B., Uusitalo, R., Withers, P., 2015. Future agriculture with minimized phosphorus losses to waters: research needs and directions. *Ambio* 44 (2), S163–S179.

Shore, M., Murphy, S., Mellander, P., Shortle, G., Melland, A.R., Crockford, L., O'Flaherty, V., Williams, L., Morgan, G., Jordan, P., 2017. Influence of stormflow and baseflow phosphorus pressures on stream ecology in agricultural catchments. *Sci. Total Environ.* 590–591, 469–483.

Smith, D.R., King, K.W., Williams, M.R., 2015. What is causing the harmful algal blooms in Lake Erie? *J. Soil Water Conserv.* 70, 27A–29A.

Stow, C.A., Cha, Y., Johnson, L.T., Confesor, R., Richards, R.P., 2015. Long-term and seasonal trend decomposition of Maumee River nutrient inputs to western Lake Erie. *Environ. Sci. Technol.* 49 (6), 3392–3400.

U.S. EPA, 1983. *Methods for Chemical Analysis of Water and Wastes*. EPA 600/4-79-02. US Environmental Protection Agency, Environmental Monitoring and Support Laboratory, Cincinnati, OH.

U.S. Environmental Protection Agency, 2017. Discharge Monitoring Report Pollution Loading Tool [https://cfpub.epa.gov/dmr/facility\\_search.cfm](https://cfpub.epa.gov/dmr/facility_search.cfm).

Venier, M., Hung, H., Tych, W., Hites, R.A., 2012. Temporal trends of persistent organic pollutants: a comparison of different time series models. *Environ. Sci. Technol.* 46, 3928–3934.

Wang, S., Jin, X., Bu, Q., Jiao, L., Wu, F., 2008. Effects of dissolved oxygen supply level on phosphorus release from lake sediments. *Colloids Surf. A* 316, 245–252.

Webster, J.R., Newbold, J.D., Lin, L., 2016. Nutrient spiraling and transport in streams—the importance of in stream biological processes to nutrient dynamics in streams. In: Jones, J., Stanley, E. (Eds.), *Stream Ecosystems in a Changing Environment*. Elsevier, Amsterdam.

Williams, M.R., King, K.W., Fausey, N.R., 2015a. Contribution of tile drains to basin discharge and nitrogen export in a headwater agricultural watershed. *Agric. Water Manage.* 158, 42–50.

Williams, M.R., King, K.W., Fausey, N.R., 2015b. Drainage water management effects on tile discharge and water quality. *Agric. Water Manage.* 148, 43–51.

Williams, M., King, K., Ford, W., Buda, A., Kennedy, C., 2016. Effect of tillage on macropore flow and phosphorus transport to tile drains. *Wat. Resour. Res.* 52, 2868–2882. <https://doi.org/10.1002/2015WR017650>.

Wu, Z., Huang, N.E., 2004. A study of the characteristics of white noise using the empirical mode decomposition method. *Proc. R. Soc. Lond.* 460 (2046), 1567–1611.

Wu, Z., Huang, N.E., Peng, C., 2007. On the trend, detrending, and variability of nonlinear and nonstationary time series. *Proc. Natl. Acad. Sci. USA* 104 (38), 14889–14894.

Wu, Y., Wen, Y., Zhou, J., Wu, Y., 2014. Phosphorus release from lake sediments: effects of pH, temperature and dissolved oxygen. *KSCE J. Civ. Eng.* 18 (1), 323–329.